

Counterclockwise Dynamics of a Rate-Independent Semilinear Duhem Model

Ashwani K. Padthe, JinHyoungh Oh, and Dennis S. Bernstein

Department of Aerospace Engineering, The University of Michigan,
Ann Arbor, MI 48109-2140, USA, {akpadthe, johzz, dsbaero}@umich.edu

Abstract—Counterclockwise hysteresis maps are known to be dissipative in the energy sense as well as in the system-theoretic sense. In a recent paper, Angeli studied feedback interconnections of counterclockwise systems, where counterclockwise refers to the net signed area of the input-output map, which need not be a simple closed curve. In the present paper we apply this notion to the study of hysteretic models. In particular, we give conditions under which the semilinear Duhem model is counterclockwise.

I. INTRODUCTION

In structural analysis, damping characteristics can be assessed by determining the stress-strain behavior of the material [1]. Under adiabatic (thermal equilibrium) conditions, the stress-strain relationship has the form of a hysteretic simple closed curve. In magnetics, hysteresis caused by the irreversible flux-change mechanism dissipates energy in the form of heat [2]. In both cases, the energy dissipated in one cycle is equal or proportional to the area enclosed by the hysteretic map [3]–[6] under a periodic input. In these applications energy dissipativity is associated with counterclockwise traversal of the hysteresis map under cyclic inputs.

Counterclockwise traversal is also known to have a direct relationship to dissipativity in the system-theoretic sense [7]–[10]. For certain systems with counterclockwise hysteresis, it has been shown that the system is system-dissipative between the input and the derivative of the output, that is, between u and \dot{y} . Under various assumptions, this property was proved in [11] as well as in [12], [13] for a class of Preisach models.

In many applications involving hysteresis, the hysteresis map is not simple, but rather is self crossing. These *butterfly* or *X-type* hysteresis maps arise in electromagnetics [14], [15], piezo materials [16], [17], and optics [18]–[20]. For such systems it is of interest to determine both energy-dissipativity and system-theoretic dissipativity.

Recently, Angeli [21] provided a characterization of system dissipativity in terms of the counterclockwise behavior of the input-output map. Specifically, a dynamical system is defined to be *counterclockwise* if

$$\liminf_{t \rightarrow \infty} \int_0^t \{\dot{y}^T(s)u(s) - \dot{u}^T(s)y(s)\} ds > -\infty,$$

for each bounded input u and the corresponding output y . This integral represents the signed area of the curve $(u(t), y(t))$ as given by Green's theorem. This definition refers to the net signed area so that the I-O map need not

be a simple closed curve. Consequently, this definition is applicable to butterfly or X-type hysteresis maps.

In the present paper we define counterclockwise in terms of periodic input signals rather than bounded inputs as in [21]. This restriction allows us to focus on the hysteresis map, which is defined to be the limiting I-O map in the quasi-static limit; for details, see [22], [23]. With this definition we show that if the (u, \dot{y}) system is passive then the (u, y) system is counterclockwise. Next we consider the semilinear Duhem model and give sufficient conditions under which the system is counterclockwise. We also explain how the stability of a positive position feedback interconnection can be analyzed using the counterclockwise orientation analysis.

II. COUNTERCLOCKWISE DYNAMICS AND PASSIVITY

In this section we define counterclockwise I-O dynamics and passivity of a system, and then consider the relationship between these properties. Consider the input-output system

$$\dot{x}(t) = f(x(t), u(t), \dot{u}(t)), \quad x(0) = x_0, \quad t \geq 0, \quad (1)$$

$$y(t) = h(x(t), u(t)), \quad (2)$$

where $f : \mathbb{R}^n \times \mathbb{R}^m \times \mathbb{R}^m \rightarrow \mathbb{R}^n$, $h : \mathbb{R}^n \times \mathbb{R}^m \rightarrow \mathbb{R}^m$, $x \in \mathbb{R}^n$, $u \in \mathbb{R}^m$, and $y \in \mathbb{R}^m$. We begin by recalling the classical Green's theorem [24].

Theorem 2.1: Let \mathcal{C} be a positively oriented, piecewise-smooth, simple closed curve in the plane and let \mathcal{D} be the region enclosed by \mathcal{C} . If $P(x, y)$ and $Q(x, y)$ have continuous partial derivatives on an open region that contains \mathcal{D} , then,

$$\int_{\mathcal{C}} P dx + Q dy = \iint_{\mathcal{D}} \left(\frac{\partial Q}{\partial x} - \frac{\partial P}{\partial y} \right) dA, \quad (3)$$

where the left hand side is a line integral along the closed curve \mathcal{C} and the right hand side is surface integral over the enclosed region \mathcal{D} .

We consider closed curves that are not necessarily simple. In particular, we consider closed curves that are the union of a finite collection of simple closed curves. For such curves, each integral in (3) is the summation of integrals evaluated over each individual simple closed curve and the corresponding enclosed region.

The convention used in Green's theorem is that the positive orientation of \mathcal{C} refers to its counterclockwise traversal, in which the enclosed region \mathcal{D} is on the left as one moves along \mathcal{C} . Now let $P(x, y) = -y/2$ and $Q(x, y) = x/2$, so that $\frac{\partial Q}{\partial x} - \frac{\partial P}{\partial y} = 1$. Then, the right hand side of (3) is the *signed*

area \mathcal{A} enclosed by the closed curve \mathcal{C} . The area evaluated using (3) is positive when the line integral is evaluated along the closed curve in a counterclockwise direction. Thus, the signed area enclosed by a closed curve is defined as follows,

Definition 2.1: Suppose that the closed curve \mathcal{C} is a finite union of simple closed curves. The *signed area* \mathcal{A} enclosed by \mathcal{C} is given by

$$\mathcal{A} \triangleq \frac{1}{2} \int_{\mathcal{C}} xdy - ydx. \quad (4)$$

The area \mathcal{A} given by (4) is the net sum of the signed contribution of each subregion enclosed by the curve \mathcal{C} . Hence, the signed area is different from the geometric area enclosed by a curve. Based on Definition 2.1 and Definition 1.1 of [21], we define a counterclockwise input-output system.

Definition 2.2: The input-output system (1), (2) is *counterclockwise* if there exists $\gamma \in \mathbb{R}$ such that, for all $x_0 \in \mathbb{R}^n$ and $T \geq 0$ and for every input-output pair (u, y) satisfying (1), (2), where $u : [0, \infty) \rightarrow [u_{\min}, u_{\max}]$ is continuous, differentiable, and periodic with period α and has exactly one local maximum u_{\max} in $[0, \alpha)$ and exactly one local minimum u_{\min} in $[0, \alpha)$, and y is bounded and differentiable,

$$\int_0^T [\dot{y}^T(s)u(s) - \dot{u}^T(s)y(s)] ds \geq \gamma. \quad (5)$$

The following definition is given in [7].

Definition 2.3: The input-output system (1), (2) is *passive* if there exists $\beta \in \mathbb{R}$ such that, for every bounded pair (u, y) satisfying (1), (2) and for all $T \geq 0$,

$$\int_0^T y^T(s)u(s)ds \geq \beta. \quad (6)$$

Remark 2.1: Note that $\beta \leq 0$, since $u(t) \equiv 0$ gives $\beta = 0$.

Now consider (1) with the output

$$z(t) = \dot{y}(t) = \frac{d}{dt}h(x(t)), \quad (7)$$

where y is given by (2). The following result shows that the (u, y) dynamics are counterclockwise if the (u, z) dynamics are passive.

Proposition 2.1: If the system (1), (7) is passive then the system (1), (2) is counterclockwise.

Proof. Consider the system (1), (2). Suppose the input $u : [0, \infty) \rightarrow [u_{\min}, u_{\max}]$ is continuous, piecewise C^1 , differentiable and periodic with period α and has exactly one local maximum u_{\max} in $[0, \alpha)$ and exactly one local minimum u_{\min} in $[0, \alpha)$, and the output y is differentiable and bounded. Note that, for all $t \geq 0$,

$$\begin{aligned} & \int_0^t \{\dot{y}^T(s)u(s) - \dot{u}^T(s)y(s)\}ds \\ &= 2 \int_0^t \dot{y}^T(s)u(s)ds - u^T(t)y(t) + u^T(0)y(0). \end{aligned}$$

Since (1), (7) is passive, there exists $\beta \in \mathbb{R}$ such that, for all $t \geq 0$,

$$\int_0^t \dot{y}^T(s)u(s)ds \geq \beta.$$

Hence, for all $t \geq 0$,

$$\begin{aligned} & \int_0^t \{\dot{y}^T(s)u(s) - \dot{u}^T(s)y(s)\}ds \\ & \geq 2\beta + u^T(0)y(0) - u^T(t)y(t). \end{aligned} \quad (8)$$

Since u and y are bounded, there exists $\eta \in \mathbb{R}$ such that, for all $t \geq 0$,

$$\begin{aligned} u^T(t)y(t) - u^T(0)y(0) & \leq \|u^T(t)y(t)\| + \|u^T(0)y(0)\| \\ & \leq \|u(t)\|\|y(t)\| + \|u(0)\|\|y(0)\| \\ & \leq 2\eta^2. \end{aligned}$$

Hence, for all $t \geq 0$,

$$u^T(0)y(0) - u^T(t)y(t) \geq -2\eta^2. \quad (9)$$

Combining (8) and (9), yields for all $t \geq 0$,

$$\int_0^t \{\dot{y}^T(s)u(s) - \dot{u}^T(s)y(s)\}ds \geq \gamma,$$

where $\gamma \triangleq 2\beta - 2\eta^2$. Hence (1), (2) is counterclockwise. \square

III. COUNTERCLOCKWISE DYNAMICS OF LTI SYSTEMS

Consider the single-input/single-output linear time invariant system

$$\dot{x}(t) = Ax(t) + Bu(t), \quad x(0) = x_0, \quad t \geq 0, \quad (10)$$

$$y(t) = Cx(t) + Du(t), \quad (11)$$

where $x \in \mathbb{R}^n$, $u \in \mathbb{R}$, and $y \in \mathbb{R}$. This section gives a necessary and sufficient condition for the system (10), (11) to be counterclockwise. The following result is given in [21].

Theorem 3.1: Let $G(s) \triangleq C(sI - A)^{-1}B + D$ be asymptotically stable. The system (10), (11) is counterclockwise if and only if $\angle G(j\omega) \in [-\pi, 0]$ for all $\omega \geq 0$.

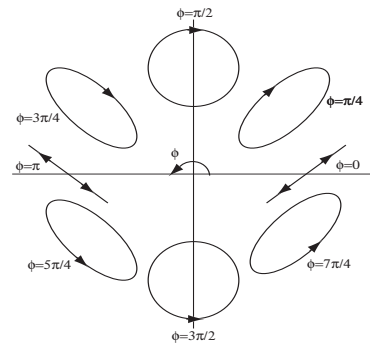


Fig. 1. Relationship between the phase angle $\phi = \angle G(j\omega)$ and the orientation of the input-output map for linear systems

Figure 1 illustrates the relationship between the phase angle $\phi = \angle G(j\omega)$ and the orientation of the I-O map.

Example 3.1: Consider the system (10), (11). Let $u(t) = \sin \omega t$, $t \geq 0$. Then, the steady state output is of the form $y(t) = \sin(\omega t + \phi)$, where ϕ is the phase angle. Then, $u(t)\dot{y}(t) = \omega \sin \omega t \cos(\omega t + \phi) = \frac{\omega}{2} \sin(2\omega t + \phi) - \frac{\omega}{2} \sin \phi$, and $\dot{u}(t)y(t) = \omega \cos \omega t \sin(\omega t + \phi) = \frac{\omega}{2} \sin(2\omega t +$

$\phi) + \frac{\omega}{2} \sin \phi$, which yields, $\int_0^t [u(s)\dot{y}(s) - \dot{u}(s)y(s)]ds = -\omega \sin \phi \int_0^t dt = -\omega t \sin \phi$. Hence,

$$\begin{aligned} & \int_0^t (\dot{y}^T(s)u(s) - \dot{u}^T(s)y(s)) ds \\ &= \begin{cases} t|\omega \sin \phi|, & \text{if } \phi \in [-\pi, 0], \\ -t|\omega \sin \phi|, & \text{if } \phi \in (0, \pi). \end{cases} \end{aligned}$$

The integral is lower bounded for all $t \geq 0$ if and only if $\phi \in [-\pi, 0]$.

Example 3.2: Consider the *compliance* transfer function (force input/position output) $G_c(s) \triangleq \frac{1}{ms^2+cs+k}$ and the *admittance* transfer function (force input/velocity output) $G_a(s) \triangleq \frac{s}{ms^2+cs+k}$. Since

$$\begin{aligned} G_c(j\omega) &= \frac{1}{-m\omega^2 + jc\omega + k} \\ &= \frac{-m\omega^2 + k}{(-m\omega^2 + k)^2 + c^2\omega^2} - j \frac{c\omega}{(-m\omega^2 + k)^2 + c^2\omega^2}, \end{aligned}$$

it follows that $\text{Im}[G_c(j\omega)] < 0$ and thus $\angle G_c(j\omega) \in [-\pi, 0]$ for all $\omega \geq 0$. Therefore, it follows from Theorem 3.1 that the compliance $G_c(s)$ is counterclockwise. However, $G_c(s)$ is not passive, since it is not positive real. On the other hand, $G_a(s)$ is positive real and thus $\angle G_a(j\omega) \in [-\frac{\pi}{2}, \frac{\pi}{2}]$ for all $\omega \geq 0$, which implies from Theorem 1 that $G_a(s)$ is *not* counterclockwise. However, it is clear that $G_a(s)$ is positive real and thus is passive. Hence, the compliance $G_c(s)$ of the m - c - k system is counterclockwise but not passive, whereas admittance $G_a(s)$ is passive but not counterclockwise. These properties are consistent with the result of Proposition 2.1 that if the (u, \dot{y}) system is passive, then the (u, y) system is counterclockwise.

IV. STABILITY OF POSITIVE POSITION FEEDBACK SYSTEMS

Positive position feedback control is a widely used technique for active structural control [25]–[27]. This technique was developed in [25] for dealing with the stability problem caused by actuator dynamics in colocated control of flexible structures. Consider the second-order scalar system with second-order actuator dynamics connected through positive position feedback given by

$$\ddot{\phi}(t) + \beta_s \dot{\phi}(t) + \omega_s^2 \phi(t) = \omega_s^2 \gamma \eta(t), \quad (12)$$

$$\ddot{\eta}(t) + \beta_a \dot{\eta}(t) + \omega_a^2 \eta(t) = \omega_a^2 \phi(t), \quad (13)$$

where $\gamma, \beta_s, \beta_a > 0$, and $\phi(t)$ and $\eta(t)$ are the scalar structure and actuator states, respectively. It was shown in [25], using the Routh-Hurwitz criterion, that the system and actuator dynamics given by (12) and (13) are stable if and only if $\gamma < 1$.

In this section we analyze the positive position feedback system (12), (13) using the orientation analysis developed in the previous sections. To do this, we first state the following lemma on positive feedback interconnections of stable linear systems with counterclockwise I-O dynamics given in [21]. A stable linear system with transfer function $G(j\omega)$ is said

to have *strictly counterclockwise I-O dynamics* if $\angle G(j\omega) \in (-\pi, 0)$ for all $\omega > 0$.

Lemma 4.1: Consider the asymptotically stable SISO linear systems

$$\dot{x}_1 = A_1 x_1 + B_1 u_1, \quad y_1 = C_1 x_1, \quad (14)$$

and

$$\dot{x}_2 = A_2 x_2 + B_2 u_2, \quad y_2 = C_2 x_2, \quad (15)$$

connected in feedback with

$$u_1 = y_2, \quad u_2 = y_1. \quad (16)$$

Assume further that one of the systems has counterclockwise and the other has strictly counterclockwise I-O dynamics. Then, the system is asymptotically stable if and only if

$$C_1 A_1^{-1} B_1 C_2 A_2^{-1} B_2 < 1. \quad (17)$$

By applying Lemma 4.1 to (12), (13) we obtain the following result.

Theorem 4.1: The system-actuator dynamics of (12) and (13) are asymptotically stable if and only if $\gamma < 1$.

Proof. We first rewrite (12) and (13) in the form (14)-(16), where

$$A_1 = \begin{bmatrix} 0 & 1 \\ -\omega_s^2 & -\beta_s \end{bmatrix}, B_1 = \begin{bmatrix} 0 \\ \omega_s^2 \gamma \end{bmatrix}, C_1 = [1 \quad 0], \quad (18)$$

$$A_2 = \begin{bmatrix} 0 & 1 \\ -\omega_a^2 & -\beta_a \end{bmatrix}, B_2 = \begin{bmatrix} 0 \\ \omega_a^2 \end{bmatrix}, C_2 = [1 \quad 0], \quad (19)$$

$$u_1 = y_2 = \eta(t), \quad \text{and} \quad u_2 = y_1 = \phi(t). \quad (20)$$

The system and actuator transfer functions are $G_s(j\omega) = \frac{\omega_s^2 \gamma}{(\omega_s^2 - \omega^2)^2 + \beta_s^2 \omega^2} [(\omega_s^2 - \omega^2) - j\beta_s \omega]$ and $G_a(j\omega) = \frac{\omega_a^2}{(\omega_a^2 - \omega^2)^2 + \beta_a^2 \omega^2} [(\omega_a^2 - \omega^2) - j\beta_a \omega]$, respectively. Since, $\text{Im}[G_s(j\omega)]$ and $\text{Im}[G_a(j\omega)]$ are negative for all $\omega > 0$, both the system and the actuator have strictly counterclockwise I-O dynamics. In the case when $\beta_a = 0$ we have, $\text{Im}[G_a(j\omega)] = 0$ and hence, $\angle G_a(j\omega) \in [-\pi, 0]$ for all $\omega \geq 0$, which implies that the actuator has counterclockwise I-O dynamics. Next we have,

$$C_1 A_1^{-1} B_1 = [1 \quad 0] \begin{bmatrix} 0 & 1 \\ -\omega_s^2 & -\beta_s \end{bmatrix}^{-1} \begin{bmatrix} 0 \\ \omega_s^2 \gamma \end{bmatrix} = -\gamma,$$

$$C_2 A_2^{-1} B_2 = [1 \quad 0] \begin{bmatrix} 0 & 1 \\ -\omega_a^2 & -\beta_a \end{bmatrix}^{-1} \begin{bmatrix} 0 \\ \omega_a^2 \end{bmatrix} = -1,$$

$$\text{and, } C_1 A_1^{-1} B_1 C_2 A_2^{-1} B_2 = \gamma.$$

Hence, it follows from Lemma 4.1 that the system-actuator feedback interconnection given in (12) and (13) is stable if and only if $\gamma < 1$. \square

V. COUNTERCLOCKWISE DYNAMICS OF A
RATE-INDEPENDENT SEMILINEAR DUHEM MODEL

We now develop a sufficient condition for a *rate-independent semilinear Duhem model* to be counterclockwise. Consider the rate-independent semilinear Duhem model

$$\dot{x}(t) = [\dot{u}_+(t)I_n \quad \dot{u}_-(t)I_n] \times \left(\begin{bmatrix} A_+ \\ A_- \end{bmatrix} x(t) + \begin{bmatrix} B_+ \\ B_- \end{bmatrix} u(t) + \begin{bmatrix} E_+ \\ E_- \end{bmatrix} \right), \quad (21)$$

$$y(t) = Cx(t) + Du(t), \quad x(0) = x_0, \quad t \geq 0, \quad (22)$$

where $A_+ \in \mathbb{R}^{n \times n}$, $A_- \in \mathbb{R}^{n \times n}$, $B_+ \in \mathbb{R}^n$, $B_- \in \mathbb{R}^n$, $E_+ \in \mathbb{R}^n$, $E_- \in \mathbb{R}^n$, $C \in \mathbb{R}^{1 \times n}$, $D \in \mathbb{R}$, and

$$\dot{u}_+(t) \triangleq \max\{0, \dot{u}(t)\}, \quad \dot{u}_-(t) \triangleq \min\{0, \dot{u}(t)\}. \quad (23)$$

As shown in [23], the rate-independent semilinear Duhem model (21) and (22) can be reparameterized in terms of u as

$$\frac{d\hat{x}(u)}{du} = \begin{cases} A_+\hat{x}(u) + B_+u + E_+, & \text{when } u \text{ increases,} \\ A_-\hat{x}(u) + B_-u + E_-, & \text{when } u \text{ decreases,} \\ 0, & \text{otherwise,} \end{cases}$$

$$\hat{y}(u) = C\hat{x}(u) + Du,$$

where $u \in [u_{\min}, u_{\max}]$ with initial condition $\hat{x}(u_0) = x_0$.

In the following development, we refer to the limiting I-O map \mathcal{F}_∞ and hysteresis map \mathcal{H}_∞ defined in [23]. Furthermore, let A^D denote the Drazin generalized inverse of A , $\text{ind } A$ denote the index of A [28, p. 122], and $\rho(A)$ denote the spectral radius of $A \in \mathbb{R}^{n \times n}$. The following result given in [23] provides a sufficient condition for the existence of the limiting periodic I-O map of a rate-independent semilinear Duhem model.

Theorem 5.1: Consider the rate-independent semilinear Duhem model (21), (22), where $u : [0, \infty) \rightarrow [u_{\min}, u_{\max}]$ is continuous, piecewise C^1 , and periodic with period α and has exactly one local maximum u_{\max} in $[0, \alpha)$ and exactly one local minimum u_{\min} in $[0, \alpha)$. Furthermore, define $\sigma \triangleq u_{\max} - u_{\min}$ and assume that $\rho(e^{\sigma A_+} e^{-\sigma A_-}) < 1$. Then, (21) has a unique periodic solution $x : [0, \infty) \rightarrow \mathbb{R}^n$, the limiting periodic input-output map $\mathcal{H}_\infty(u)$ exists, and the limiting input-output map $\mathcal{F}_\infty(u, y)$ is given by $\mathcal{F}_\infty(u, y) = \mathcal{H}_\infty(u)$. Specifically,

$$\mathcal{H}_\infty(u) = \left\{ (u, \hat{y}_+(u)) \in \mathbb{R}^2 : u \in [u_{\min}, u_{\max}] \right\} \cup \left\{ (u, \hat{y}_-(u)) \in \mathbb{R}^2 : u \in [u_{\min}, u_{\max}] \right\}, \quad (24)$$

where

$$\hat{y}_+(u) = Ce^{A_+(u-u_{\min})}\hat{x}_+ + C\mathcal{X}_+(u, u_{\min}) + C\mathcal{Y}_+(u - u_{\min}) - C\mathcal{Z}_+(u, u_{\min}) + Du, \quad (25)$$

$$\hat{y}_-(u) = Ce^{A_-(u-u_{\max})}\hat{x}_- + C\mathcal{X}_-(u, u_{\max}) + C\mathcal{Y}_-(u - u_{\max}) - C\mathcal{Z}_-(u, u_{\max}) + Du, \quad (26)$$

and

$$\hat{x}_+ \triangleq (I - e^{-\sigma A_-} e^{\sigma A_+})^{-1} (e^{-\sigma A_-} \mathcal{W}_+ + \mathcal{W}_-),$$

$$\hat{x}_- \triangleq (I - e^{\sigma A_+} e^{-\sigma A_-})^{-1} (e^{\sigma A_+} \mathcal{W}_- + \mathcal{W}_+),$$

$$\mathcal{W}_+ \triangleq \mathcal{X}_+(u_{\max}, u_{\min}) + \mathcal{Y}_+(\beta) - \mathcal{Z}_+(u_{\max}, u_{\min}),$$

$$\mathcal{W}_- \triangleq \mathcal{X}_-(u_{\min}, u_{\max}) + \mathcal{Y}_-(-\beta) - \mathcal{Z}_-(u_{\min}, u_{\max}),$$

$$\mathcal{X}_+(u, u_0) \triangleq (I - A_+ A_+^D) \sum_{k=1}^{r_+} \frac{u + ku_0}{(k+1)!} (u - u_0)^k A_+^{k-1} B_+,$$

$$\mathcal{X}_-(u, u_0) \triangleq (I - A_- A_-^D) \sum_{k=1}^{r_-} \frac{u + ku_0}{(k+1)!} (u - u_0)^k A_-^{k-1} B_-,$$

$$\mathcal{Y}_+(u) \triangleq (I - A_+ A_+^D) \sum_{k=1}^{r_+} \frac{1}{k!} u^k A_+^{k-1} E_+,$$

$$\mathcal{Y}_-(u) \triangleq (I - A_- A_-^D) \sum_{k=1}^{r_-} \frac{1}{k!} u^k A_-^{k-1} E_-,$$

$$\mathcal{Z}_+(u, u_0) \triangleq A_+^D (uI - u_0 e^{A_+(u-u_0)}) B_+ + A_+^{2D} \times (I - e^{A_+(u-u_0)}) B_+ + A_+^D (I - e^{A_+(u-u_0)}) E_+,$$

$$\mathcal{Z}_-(u, u_0) \triangleq A_-^D (uI - u_0 e^{A_-(u-u_0)}) B_- + A_-^{2D} \times (I - e^{A_-(u-u_0)}) B_- + A_-^D (I - e^{A_-(u-u_0)}) E_-.$$

For the following results, $\oint_{\mathcal{H}_\infty(u)}$ indicates line integral evaluated along the hysteresis loop $\mathcal{H}_\infty(u)$. Furthermore, $\hat{y}_+(u)$ and $\hat{y}_-(u)$ are given by (25) and (26), respectively.

Proposition 5.1: Consider the rate-independent semilinear Duhem model (21), (22), where $u : [0, \infty) \rightarrow [u_{\min}, u_{\max}]$ is continuous, differentiable, and periodic with period α and has exactly one local maximum u_{\max} in $[0, \alpha)$ and exactly one local minimum u_{\min} in $[0, \alpha)$. Furthermore, define $\sigma \triangleq u_{\max} - u_{\min}$ and assume that $\rho(e^{\sigma A_+} e^{-\sigma A_-}) < 1$. Then, the system is counterclockwise if and only if $\oint_{\mathcal{H}_\infty(u)} \hat{y}(u) du \leq 0$. In particular, when $\mathcal{H}_\infty(u)$ is simple, the system is counterclockwise if and only if $\hat{y}_+(u) \leq \hat{y}_-(u)$ for all $u \in [u_{\min}, u_{\max}]$.

Proof. Since, $\rho(e^{\beta A_+} e^{-\beta A_-}) < 1$ and $u : [0, \infty) \rightarrow [u_{\min}, u_{\max}]$ is continuous, differentiable, and periodic with period α and has exactly one local maximum u_{\max} in $[0, \alpha)$ and exactly one local minimum u_{\min} in $[0, \alpha)$, Theorem 5.1 states that the limiting periodic input-output map $\mathcal{H}_\infty(u)$ given by (24) exists. Now, note that, for all $t \geq 0$,

$$\int_0^t [\dot{y}(s)u(s) - \dot{u}(s)y(s)] ds = u(t)y(t) - u(0)y(0) - 2 \int_0^t \dot{u}(s)y(s) ds. \quad (27)$$

The integral on the right hand side of (27) can be written as

$$\int_0^t \dot{u}(s)y(s) ds = \int_{u_0}^{u_t} \hat{y}(u) du = \alpha + \beta \oint_{\mathcal{H}_\infty(u)} \hat{y}(u) du \quad (28)$$

where $u_0 = u(0)$, $u_t = u(t)$, $\alpha, \beta \in \mathbb{R}$, $\beta \geq 0$ is the number of complete traversals along $\mathcal{H}_\infty(u)$ on $[0, t]$, and α accounts for the transients and incomplete traversals. Hence,

combining (27) and (28),

$$\begin{aligned} & \int_0^t [\dot{y}(s)u(s) - \dot{u}(s)y(s)] ds \\ &= u(t)y(t) - u(0)y(0) - 2\alpha - 2\beta \oint_{\mathcal{H}_\infty(u)} \hat{y}(u) du. \end{aligned} \quad (29)$$

Since, u and y are bounded,

$$\int_0^t [\dot{y}(s)u(s) - \dot{u}(s)y(s)] ds = \eta(t) - 2\beta \oint_{\mathcal{H}_\infty(u)} \hat{y}(u) du. \quad (30)$$

where $\eta(t) \triangleq u(t)y(t) - u(0)y(0) - 2\alpha$ is a scalar.

To prove sufficiency, note that $\beta \rightarrow \infty$ as $t \rightarrow \infty$. Now, if $\oint_{\mathcal{H}_\infty(u)} \hat{y}(u) du \leq 0$, then $\int_0^t (\dot{y}(s)u(s) - \dot{u}(s)y(s)) ds \rightarrow \infty$, that is, the integral on the left hand side of (30) is lower bounded for all $t \geq 0$. Hence, the system is counterclockwise.

To prove necessity, assume that (21), (22) is counterclockwise. That is, there exists $\gamma \in \mathbb{R}$, such that

$$\int_0^t [\dot{y}(s)u(s) - \dot{u}(s)y(s)] ds \geq \gamma. \quad (31)$$

Combining (30) and (31) implies that

$$-2\beta \oint_{\mathcal{H}_\infty(u)} \hat{y}(u) du \geq \gamma - \eta(t). \quad (32)$$

Since, $\beta \rightarrow \infty$ as $t \rightarrow \infty$, the inequality (32) holds for all $t \geq 0$ only if $\oint_{\mathcal{H}_\infty(u)} \hat{y}(u) du \leq 0$. Now,

$$\begin{aligned} \int_{\mathcal{H}_\infty(u)} \hat{y}(u) du &= \int_{u_{\min}}^{u_{\max}} \hat{y}_+(u) du + \int_{u_{\max}}^{u_{\min}} \hat{y}_-(u) du \\ &= \int_{u_{\min}}^{u_{\max}} \hat{y}_+(u) du - \int_{u_{\min}}^{u_{\max}} \hat{y}_-(u) du \\ &= \int_{u_{\min}}^{u_{\max}} (\hat{y}_+(u) - \hat{y}_-(u)) du. \end{aligned}$$

If the hysteresis loop $\mathcal{H}_\infty(u)$ is simple, then the difference $\hat{y}_+(u) - \hat{y}_-(u)$ has the same sign for all $u \in (u_{\min}, u_{\max})$. Hence, $\oint_{\mathcal{H}_\infty(u)} \hat{y}(u) du \leq 0$ if and only if $\hat{y}_+(u) \leq \hat{y}_-(u)$ for all $u \in (u_{\min}, u_{\max})$. \square

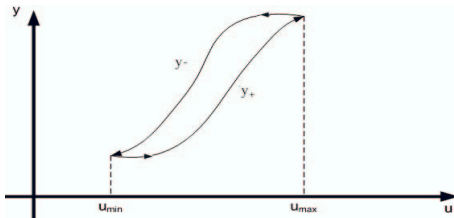


Fig. 2. Illustration of $y_- \geq y_+$ for a simple counterclockwise closed curve.

Proposition 5.2: Consider the rate-independent semi-linear Duhem model (21), (22), where $u : [0, \infty) \rightarrow [u_{\min}, u_{\max}]$ is continuous, differentiable, and periodic with period α and has exactly one local maximum u_{\max} in $[0, \alpha)$ and exactly one local minimum u_{\min} in $[0, \alpha)$. Furthermore,

define $\sigma \triangleq u_{\max} - u_{\min}$ and assume that $\rho(e^{\sigma A_+} e^{-\sigma A_-}) < 1$. If $\hat{y}_+(u)$ is concave and $\hat{y}_-(u)$ is convex or, equivalently,

$$\frac{d^2 \hat{y}_+(u)}{du^2} > 0, \quad \frac{d^2 \hat{y}_-(u)}{du^2} < 0, \quad (33)$$

for all $u \in (u_{\min}, u_{\max})$, then, $\mathcal{H}_\infty(u)$ is simple and the system is counterclockwise.

Proof. Let $u : [0, \infty) \rightarrow [u_{\min}, u_{\max}]$ be continuous, differentiable, and periodic with period α and have exactly one local maximum u_{\max} in $[0, \alpha)$ and exactly one local minimum u_{\min} in $[0, \alpha)$. Assuming $\rho(e^{\sigma A_+} e^{-\sigma A_-}) < 1$, where $\sigma \triangleq u_{\max} - u_{\min}$, Theorem 5.1 tells us that the limiting periodic input-output map $\mathcal{H}_\infty(u)$ given by (24) exists. To begin with, assume that $\mathcal{H}_\infty(u)$ is simple and satisfies (33). As illustrated in Figure 3, define

$$\begin{aligned} y_1 &\triangleq \hat{y}_+(u_{\min}) = \hat{y}_-(u_{\min}), \\ y_2 &\triangleq \hat{y}_+(u_{\max}) = \hat{y}_-(u_{\max}). \end{aligned}$$

Without loss of generality, it can be assumed that,

$$y_1 \leq y_2. \quad (34)$$

Since, $\hat{y}_+(u)$ is concave, let $u = u^*$ be a local minimizer of \hat{y}_+ . Hence,

$$\hat{y}_+(u^*) < y_1 \leq y_2. \quad (35)$$

Now, since $\hat{y}_-(u)$ is convex, its minimum value occurs at the end points, that is, either at $u = u_{\min}$ or at $u = u_{\max}$. Hence, using (34), $\min_{u \in [u_{\min}, u_{\max}]} (\hat{y}_-(u)) = y_1$, which implies that,

$$y_1 < \hat{y}_-(u^*). \quad (36)$$

Combining (35) and (36) yields

$$\hat{y}_+(u^*) < \hat{y}_-(u^*). \quad (37)$$

For a simple closed loop, the difference $\hat{y}_+ - \hat{y}_-$ does not change sign over the range $u \in (u_{\min}, u_{\max})$. Hence, for all $u \in (u_{\min}, u_{\max})$,

$$\hat{y}_+(u) - \hat{y}_-(u) \leq 0, \quad (38)$$

which implies that the simple closed loop is counterclockwise. If the hysteresis loop $\mathcal{H}_\infty(u)$ is not simple, then it can be expressed as the union of a finite collection of simple closed sub-loops. By applying the above analysis to each of the simple closed sub-loops separately, it follows that every loop is counterclockwise. But, this is not possible. Two adjacent interconnected simple closed loops cannot have the same orientation (Figure 4). Therefore, the hysteresis loop $\mathcal{H}_\infty(u)$ has to be a simple closed curve and satisfy (38), which, according to Proposition 5.1 is equivalent to the system being counterclockwise. \square

Remark 5.1: For the semi-linear Duhem model (21), (22), the concavity-convexity conditions (33) are equivalent to

$$O_+(u) = CA_+^2 \hat{x}(u) + CA_+ B_+ u + CB_+ + CA_+ E_+ > 0, \quad (39)$$

$$O_-(u) = CA_-^2 \hat{x}(u) + CA_- B_- u + CB_- + CA_- E_- < 0. \quad (40)$$

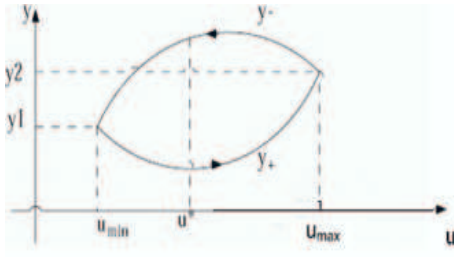


Fig. 3. Illustration of $y_- \geq y_+$ for a simple closed curve when y_- is convex and y_+ is concave.

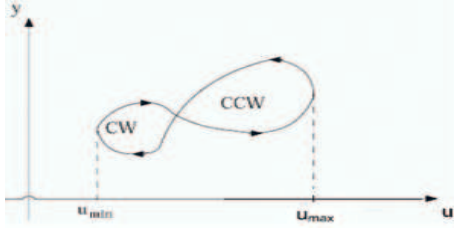


Fig. 4. Illustration of the fact that two adjacent interconnected closed loops cannot both be counterclockwise.

Example 5.1: Consider the semilinear Duhem model

$$\begin{aligned} \dot{x}(t) &= [\dot{u}_+(t) \quad \dot{u}_-(t)] \left(\begin{bmatrix} -1 \\ 1 \end{bmatrix} x(t) + \begin{bmatrix} b \\ -b \end{bmatrix} u(t) \right), \\ y(t) &= x(t), \quad x(0) = 0, \quad t \geq 0. \end{aligned}$$

Let $u(t) = \sin t$, $t \geq 0$. If $b = 1$, then it can be seen by solving numerically that $\mathcal{O}_+(u) > 0$ and $\mathcal{O}_-(u) < 0$ for all $u \in [-1, 1]$. Hence, it follows from Proposition 5.2 that the hysteresis loop is simple and the system is counterclockwise, as shown in Figure 5(a). Alternatively, if $b = -1$, then it can be seen that $\mathcal{O}_+(u) < 0$ and $\mathcal{O}_-(u) > 0$ for all $u \in [-1, 1]$. As shown in Figure 5(b), the system is not counterclockwise.

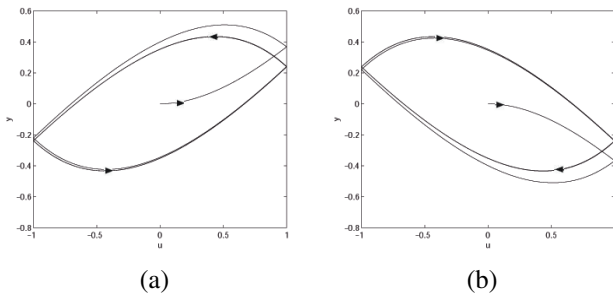


Fig. 5. The input-output map of Example 5.1 with (a) $b = 1$, the orientation is counterclockwise, (b) $b = -1$, the orientation is clockwise.

VI. CONCLUSION

In this paper we related the counterclockwise-ness and passivity of a nonlinear input-output system. We then developed a sufficient condition for a rate-independent semilinear Duhem model to be counterclockwise. These results will be useful in studying the behavior of feedback interconnections of hysteretic systems. We also explained how the stability of

a positive position feedback interconnection can be studied using counterclockwise orientation analysis.

REFERENCES

- [1] A. D. Nashif, D. I. G. Jones, and J. P. Henderson, *Vibration Damping*. New York: Wiley, 1985.
- [2] J. B. Goodenough, "Summary of losses in magnetic materials," *IEEE Trans. Magnetics*, vol. 38, no. 5, pp. 3398–3408, 2002.
- [3] W.W.Soroka, "Note on the relations between viscous and structural damping coefficients," *J. Aeronautical Sciences*, vol. 16, pp. 409–410, 1949.
- [4] W. C. Hurty and M. F. Rubinstein, *Dynamics of Structures*. Englewood Cliffs, NJ: Prentice Hall, 1964.
- [5] L. Meirovitch, *Analytical Methods in Vibrations*. McMillan, 1967.
- [6] I. D. Mayergoyz, *Mathematical Models of Hysteresis*. New York: Springer-Verlag, 1991.
- [7] R. Lozano, B. Brogliato, O. Egeland, and B. Maschke, *Dissipative Systems Analysis and Control: Theory and Applications*. London, Great Britain: Springer-Verlag, 2000.
- [8] J. C. Willems, "Dissipative dynamical systems part I: General theory," *Arch. Rational Mech. Anal.*, vol. 45, pp. 321–351, 1972.
- [9] P. J. Moylan, "Implications of passivity in a class of nonlinear systems," *IEEE Trans. Autom. Contr.*, vol. 19, pp. 373–381, 1974.
- [10] D. J. Hill and P. J. Moylan, "Stability results for nonlinear feedback systems," *Automatica*, vol. 13, pp. 377–382, 1977.
- [11] T. Paré, A. Hassabi, and J. J. How, "A KYP lemma and invariance principle for systems with multiple hysteresis non-linearities," *Int. J. Contr.*, vol. 74, no. 11, pp. 1140–1157, 2001.
- [12] R. B. Gorbet, K. A. Morris, and D. W. L. Wang, "Control of hysteretic systems: A state space approach," in *Learning, Control and Hybrid Systems*. New York: Springer, 1998, pp. 432–451.
- [13] R. B. Gorbet and K. A. Morris, "Generalized dissipation in hysteretic systems," in *Proc. IEEE Conf. Dec. Contr.*, 1998, pp. 4193–4198.
- [14] J. A. Barker, D. E. Schreiber, B. G. Huth, and D. H. Everett, "Magnetic hysteresis and minor loops: Models and experiments," *Proc. the Royal Society of London*, vol. A386, pp. 251–261, 1983.
- [15] P. J. Chen and S. T. Montgomery, "A macroscopic theory for the existence of the hysteresis and butterfly loops in ferroelectricity," *Ferroelectrics*, vol. 23, no. 3–4, pp. 199–208, 1980.
- [16] U. von Wagner, "Non-linear longitudinal vibrations of non-slender piezoceramic rods," *Int. J. Non-Linear Mech.*, vol. 39, pp. 673–688, 2004.
- [17] U. von Wagner and P. Hagedorn, "Nonlinear effects of piezoceramics excited by weak electric fields," *Nonlinear Dyn.*, vol. 31, pp. 133–149, 2003.
- [18] N. F. Mitchell, J. O’Gorman, J. Hegarty, and J. C. Connolly, "Optical bistability and X-shaped hysteresis in laser diode amplifiers," in *Lasers and Electro-Optics Society Annual Meeting*, 1993, pp. 520–521.
- [19] H. M. Gibbs, *Optical Bistability: Controlling Light with Light*. Academic Press, 1985.
- [20] N. B. An and L. T. C. Tuong, "Possible hysteresis loops of resonatorless optical bistability," *Solid State Communications*, vol. 76, no. 9, pp. 1139–1142, 1990.
- [21] D. Angeli, "On systems with counterclockwise input-output dynamics," in *Proc. IEEE Conf. Dec. Contr.*, Atlantis, Bahamas, 2004, pp. 2527–2532.
- [22] J. Oh and D. S. Bernstein, "Identification of rate-dependent hysteresis using the semilinear Duhem model," in *Proc. Amer. Contr. Conf.*, Boston, MA, 2004, pp. 4776–4781.
- [23] —, "Semilinear Duhem model for rate-independent and rate-dependent hysteresis," *IEEE Trans. Autom. Contr.*, vol. 50, no. 5, pp. 631–645, 2005.
- [24] J. Stewart, *Calculus*. Pacific Grove, CA: Brooks/Cole Pub Co., 1999.
- [25] C. J. Goh and T. K. Caughey, "On the stability problem caused by finite actuator dynamics in the collocated control of large space structures," *Int. J. Contr.*, vol. 41, pp. 787–802, 1985.
- [26] M. I. Friswell and D. J. Inman, "The relationship between positive position feedback and output feedback controllers," *Smart Materials and Structures*, vol. 8, pp. 285–291, 1999.
- [27] J.-H. H. Keun-Ho Rew and I. Lee, "Multi-modal vibration control using adaptive positive position feedback," *J. Intelligent Material Syst. Struct.*, vol. 13, no. 1, pp. 13–22, 2002.
- [28] S. L. Campbell and J. C. D. Meyer, *Generalized Inverse of Linear Transformations*. London: Pitman, 1979.